

## A study of the Zn:Sn mixing ratio effect on the gas detector properties

Alaa A. Abdul-Hamead, Farhad M. Othman, Alaa S. Taeeh

Materials Engineering Department, University of Technology

E-mail: adr.alaa@yahoo.com

### Abstract

Semiconductor-based metal oxide gas detector of five mixed from zinc chloride Z and tin chloride S salts Z:S ratio 0, 25, 50, 75 and 100% were fabricated on glass substrate by a spray pyrolysis technique. With thickness were about  $0.2 \pm 0.05 \mu\text{m}$  using water soluble as precursors at a glass substrate temperature  $500 \text{ }^\circ\text{C} \pm 5$ , 0.05 M, and their gas sensing properties toward  $\text{CH}_4$ , LPG and  $\text{H}_2\text{S}$  gas at different concentration (10, 100, 1000 ppm) in air were investigated at room temperature which related with the petroleum refining industry.

Furthermore structural and morphology properties were scrutinize. Results shows that the mixing ratio affect the composition of formative oxides were ( $\text{ZnO}$ ,  $\text{Zn}_2\text{SnO}_4$ ,  $\text{Zn}_2\text{SnO}_4 + \text{ZnSnO}_3$ ,  $\text{ZnSnO}_3$ ,  $\text{SnO}_2$ ) ratios mentioned in the above respectively, and related with the sensitivity of the reduction tested gases, best sensitivity was for  $\text{H}_2\text{S}$  gas, have sensitivity about 80.61% and a response time of 10 seconds for the binary oxides and 89.57% and a response time of (5-2) seconds for the mixed ternary oxides.

### Key words

*Zinc stannate, gas sensor, ternary metal oxides, spray pyrolysis, pollutant gases, XRD.*

### Article info.

*Received: Jan. 2015*

*Accepted: Feb. 2015*

*Published: Sep. 2015*

### دراسة تأثير نسبة خلط Zn:Sn على خصائص الكاشف الغازي

آلاء علاء الدين، فرهاد محمد عثمان، آلاء صبيح تايه

قسم هندسة المواد، الجامعة التكنولوجية

### الخلاصة

في هذا البحث حضر كاشف شبه موصل اوكسيدي من خمس خلطات من أملاح كلوريد الزنك Z و كلوريد القصدير S و بنسب خلط Z:S بلغت 0, 25, 50, 75, 100% بطريقة الرش الكيميائي الحراري و بسمك حوالي  $(0.2 \pm 0.05 \mu\text{m})$  على قواعد من الزجاج و باستخدام الماء كمنظف، و بدرجات حرارة ترسيب بلغت  $500 \pm 5 \text{ }^\circ\text{C}$  و بتراكيز 0.05 M ككاشف للغازات الملوثة مثل ( $\text{CH}_4$ , LPG,  $\text{H}_2\text{S}$ ) و بتركيز (10, 100, 1000 ppm) في الهواء و بدرجة حرارة الغرفة و المرتبطة مع صناعة تكرير النفط. تم تشخيص التبلور و مورفولوجية سطح الأغشية المحضرة بواسطة قياسات حيود الأشعة السينية XRD و المجهر الإلكتروني الماسح SEM و مجهر القوة الذرية AFM لها. بينت النتائج أن نسبة خلط تؤثر على تبلور الأكاسيد المتكونة و المركبات الثلاثية المتكونة حيث كانت ( $\text{ZnO}$ ,  $\text{Zn}_2\text{SnO}_4$ ,  $\text{Zn}_2\text{SnO}_4 + \text{ZnSnO}_3$ ,  $\text{ZnSnO}_3$ ,  $\text{SnO}_2$ ) للنسب المذكورة في أعلاه على التوالي و ترتبط مع حساسية الغازات المختزلة المفحوصة، وكانت أفضل حساسية للغاز  $\text{H}_2\text{S}$  80.61% و زمن الاستجابة 10 ثانية للأكاسيد الثنائية و 89.57% و زمن الاستجابة من (2-5) ثانية لخليط الأكاسيد الثلاثية.

### Introduction

The development of high performance solid state chemical sensors is nowadays of outmost importance in many advanced technological fields[1]. One of

important application areas of gas sensor is petroleum refining industry which employs a wide variety of processes started with receipt of crude for storage at the refinery and converts

it into more than 2500 of refined products. This processes liberation large quantities of pollutants can occur as a result of abnormal operation in a refinery and potentially pose a major local environmental hazard like boilers, process heaters, and other process equipment are responsible for the emission of particulates, volatile organic compounds (VOCs). Numerous researches have shown that a characteristic of solid-state gas sensors is the reversible interaction of the gas with the surface of a solid-state material. In addition to the conductivity change of gas-sensing material, the detection of this reaction can be performed by measuring the change of capacitance, work function, mass and optical characteristics or reaction energy released by the gas/solid interaction. Various materials, synthesized in the form of porous ceramics, and deposited in the form of thick or thin films, are used as active layers in such gas-sensing devices [2]. Zinc stannate or zinc tin oxide (ZTO) is a class of ternary oxides that are known for their stable properties under extreme conditions, higher electron mobility compared to its binary counterparts and other interesting properties. The material is thus ideal for applications from, gas detector, solar cells to photocatalysts, light-emitting diodes, field effect transistors and (heterojunction and homojunction) diodes[3]. In 2001, Zakrzewska, study mixed-oxide systems such as  $\text{SnO}_2\text{-WO}_3$ ,  $\text{TiO}_2\text{-WO}_3$  and  $\text{SnO}_2\text{-TiO}_2$  with the ultimate aim of the application in gas sensing devices and study dynamic changes in the electrical resistance (R) of  $\text{SnO}_2\text{-WO}_3$  thin films for samples deposited at two different substrate temperatures, 100 and 300°C upon exposure it to hydrogen at 400°C and  $\text{CH}_4$  at 350 and 700 °C response time were more than 70 sec [3]. In 2003, Chowdhuri, et al.,

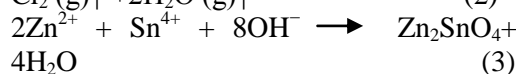
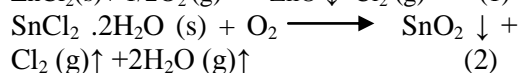
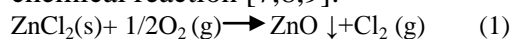
Study the response speed of  $\text{SnO}_2$  based  $\text{H}_2\text{S}$  gas sensors with CuO nanoparticles, CuO nanoparticles on sputtered  $\text{SnO}_2$  thin-film surface exhibit a fast response speed (14 sec) and recovery time 61 sec for trace level 20 ppm  $\text{H}_2\text{S}$  gas detection. The sensitivity of the sensor ( $S \sim 2.06 \times 10^3$ ) is noted to be high at a low operating temperature of 130 °C [4]. In 2004, Gong et. al., study the  $\text{SnO}_2$  nano film which was fabricated with the combination of polymeric sol-gel chemistry and block copolymers used as structure directing agents. The novel hydrogen sensor has a fast response time (2 sec) and quick recovery time (10 sec), as well as good sensitivity (up to 90), in comparing to other hydrogen sensors developed. The working temperature of the sensor developed can be reduced as low as 100 °C [5]. In 2005, Batzill, Diebold, study the surface and materials science of tin oxide and describes the physical and chemical properties that make tin oxide a suitable material for gas sensor [6]. The goals of this paper is to fabricating different semiconductor-based metal oxide gas detector of five mixed film by spray pyrolysis technique, and study some of their structural properties and sensitivity to some pollutant gases.

### Experimental work

The work includes four steps; The first step: preparation of films from an aqueous solution of zinc chloride  $\text{Z}(\text{ZnCl}_2)$  and tin chloride  $\text{S}(\text{SnCl}_2 \cdot 2\text{H}_2\text{O})$  with purities 99.9%. The concentrations was 0.05 M, salts were mixed with five weight ratios 0, 25, 50, 75 and 100% by magnetic stirrer (150 r.p.m), to study the effect of mixing ratios on the compounds formed. The acidity was maintained to be  $\approx 5.5$  pH during spraying. The preparing of the thin film is made by spray pyrolysis technique. The

spraying apparatus was manufactured locally. In this technique, the prepared aqueous solutions were atomized by a special nozzle glass sprayer at heated collector glass fixed at thermostatic controlled hot plate heater. Air was used as a carrier gas to atomize the spray solution with the help of an air compressor with pressure (7 Bar) air flow rate  $8\text{cm}^3/\text{sec}(\text{R.T})$ . The glass substrate (have thickness 0.1cm), temperature was maintained at  $500^\circ\text{C}$  during spraying.

Atomization rate was about  $1\text{nm/s}$  with  $2.5\text{ ml/min}$  of feeding rate. The distance between the collector and spray nozzle was kept at  $30 \pm 1\text{ cm}$  the volume of spray solution was  $50\text{ ml}$ , Number of spraying 100, time between two spraying 10 sec. The spray of the aqueous solution yields the following chemical reaction [7,8,9]:



where sample Z and S represent compounds  $\text{ZnCl}_2$  and  $\text{SnCl}_2 \cdot 2\text{H}_2\text{O}$  respectively.

The second step: deposition of thin film by spraying the solution on the substrate and at temperature  $500 \pm 5^\circ\text{C}$ .

The third step: After complete deposition samples, by put the samples inside annealing furnace (type nabertherm) at temperature  $500^\circ\text{C}$  for 60 min and cooling slowly inside furnace.

The Forth step: is the measurement which include:

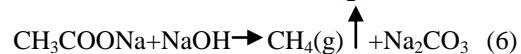
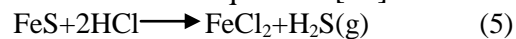
1- X-ray diffraction with diffractometer type  $\text{CuK}\alpha$  ( $\lambda = 1.5406 \text{ \AA}$ ). This test is carried out in Advanced Materials Research Center at the Technology and Science Ministry, the scanning speed was 3%.

2- Field Emission scanning electron microscopy (FE-SEM) is basically a type of electron microscope. The SEM

study has been carried out by Electron Gun Tungsten heated filament, Resolution  $3\text{ nm}$  at  $30\text{kV}$ , Accelerating voltage  $200\text{ V}$  to  $30\text{kV}$ , Chamber Internal size:  $160\text{ mm}$ , the type of coating is gold and the time of coating is  $20\text{ sec}$ , Model: TESCAN-VEGA/USA.

3- In order to observe the surface roughness and topography of deposited thin films, Atomic Force Microscopy (AFM) micrographs were taken with a Digital Instruments. Typical data has been taken from AFM height images include root mean square (RMS) and roughness. Made in USA, model AA3000 220V.

4- The gas-sensing experiments were carried out by introducing the thus prepared devices into a home-made test cell, which was consist of a cylinder with cover to restrict prepared gas as in Fig. 1. The gas was obtained from reaction solution to escalate predicted gases. Pollutant gases that prepared ( $\text{H}_2\text{S}$ ,  $\text{CH}_4$ ) will be explained in the following produce from reactions equation: [10]



LPG is a mixture largely of propane and butane and small amounts of other hydrocarbons gases[11]. This gas is called bottle gas and it's used directly to measure the sensitivity of samples, the response of samples for LPG gas is measured in site (Al-Durra refinery). The dilution were  $0.01\text{M}$  concentration, and solution was fixed at  $5\text{ml}$ , the same concentration of gases were expected to be produced. The gases -sensing properties were determined at different temperature by measurement of the D.C. electrical conductivity of the samples which was exposed to various concentration of the gases 10, 100 and  $1000\text{ ppm}_v$ . The sensor response was calculated using the following equation[12,13]:

$$\text{Sensor response}(\%) = \frac{[\text{Ra} - \text{Rg}]}{\text{Ra}} \times 100\% \quad (7)$$

where  $R_a$  and  $R_g$  are the electric.

resistance in air and test gas, respectively

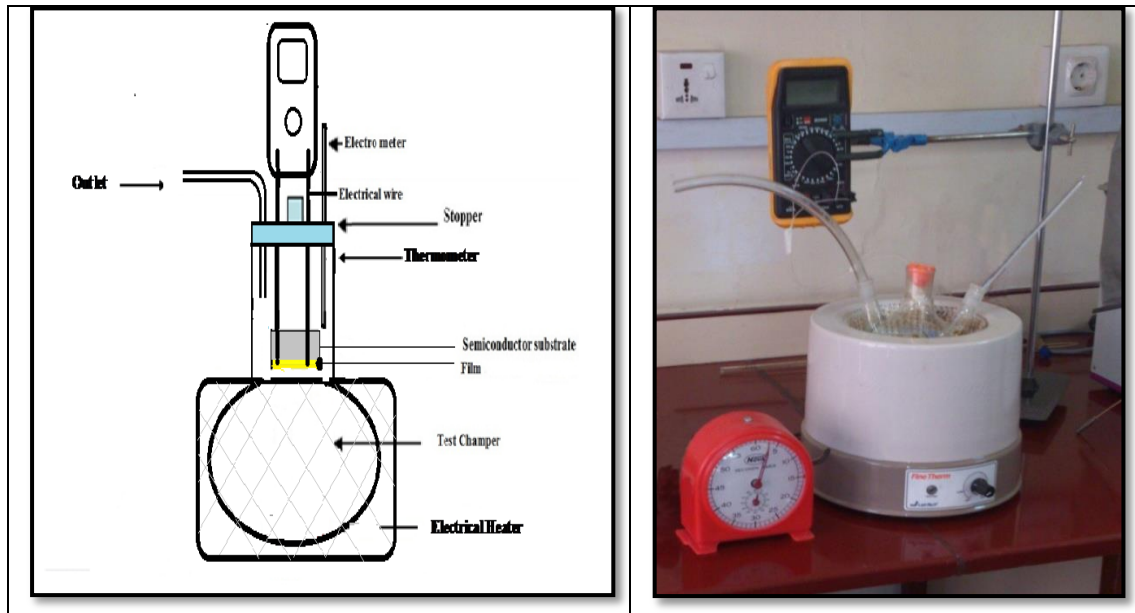


Fig. 1: Gas detection measurement system.

### Results and discussion

The results of x-ray diffraction which represent all mixing ratio (0, 25, 50, 75, 100)% for precipitation thin films on glass substrates are shown in Fig. 2. The XRD patterns result shows match with standard value in JCPDS card No. 36-1451 ZnO have wurtzite type polycrystalline thin film with a hexagonal system revealing that the highly dominant c-axis oriented film is grown, no characteristic peaks for any other impurities were observed, suggesting sample have high purity. By comparing Fig. 2 with the standard card, it's reveal that the relative intensity of the (002) diffraction peak at  $(34.409^\circ)$  much higher compared to the neighboring (100) and (101) peaks, because the growth in this orientation is higher than with other orientation, and this is consistent with many of the research for zinc oxide film [14,15].

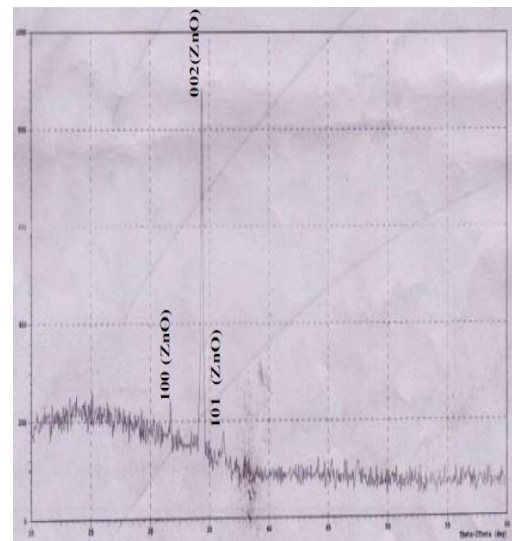


Fig. 2: XRD spectra of  $Z_1:S_0$ /glass.

In Fig. 3 it can be seen that the mixing (ZTO) of components di-zinc stannate  $Zn_2SnO_4$  and scant traces of zinc stannate  $ZnSnO_3$ , according to standard cards (JCPDS card No.24-1470 and No.28-1486) respectively. The  $Zn_2SnO_4$  have high appearance comparing with  $ZnSnO_3$  because of large accoutrement of Zn ion in mixing [16].

All of the diffraction peaks well match the standard diffraction pattern of cubic spinal structure for  $Zn_2SnO_4$ , while  $ZnSnO_3$  has a perovskite face-centered structure, coinciding with [17-19]. No diffraction peaks from any other impurities are observed. The highest intensity peak (100%) of the compound for  $Zn_2SnO_4$  is (311) at ( $2\theta=34.1384$ ). One more weak intensity peak (012) for  $ZnSnO_3$  was observed at ( $2\theta=26.3902^\circ$ ).

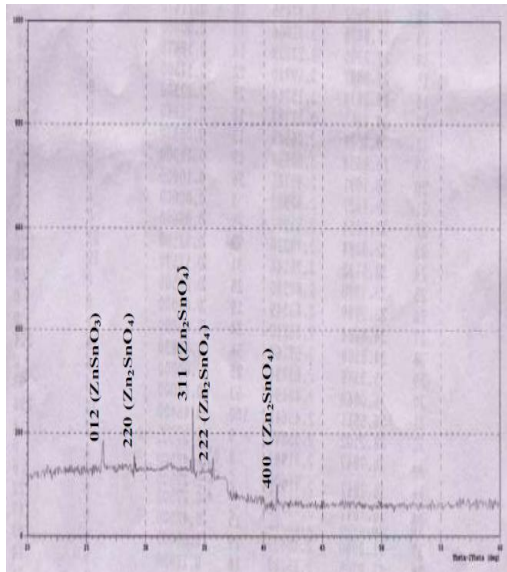


Fig. 3: XRD Spectra of  $Z_{0.75}:S_{0.25}/glass$ .

A different mixing ratio of (ZTO) is shown in Fig. 4 of components zinc stannate ( $ZnSnO_3$ ) and di-zinc stannate ( $Zn_2SnO_4$ ) return to show, by more than one peak the mixture homogenized showing deposition efficiency as well as the proper role of annealing in the formation of both two compounds according to standard cards. The 100% peak intensity belongs to  $Zn_2SnO_4$  at ( $2\theta=34.1384^\circ$ ), with orientation (311), and the 100% peak intensity belongs to  $ZnSnO_3$  at ( $2\theta=33.5053^\circ$ ), with orientation (110).

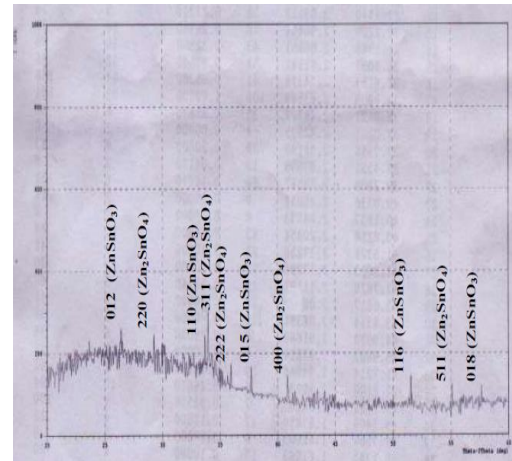


Fig.4: XRD Spectra of  $Z_{0.5}:S_{0.5}/glass$ .

Another mixing ratio ( $Z_{0.25}:S_{0.75}$ ) is shown in Fig. 5 the  $ZnSnO_3$  is appear and it has high appearance comparing with  $Zn_2SnO_4$  because of large amount of equipage of Sn ions in mixing. The highest peaks for the compound  $ZnSnO_3$ , and for  $Zn_2SnO_4$  more than one weak peaks were observed as shown in table below.

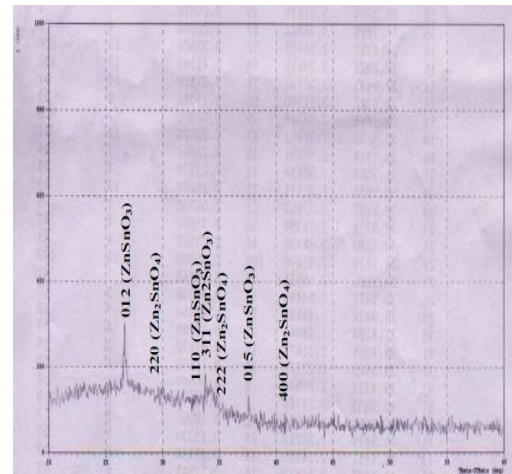


Fig. 5: XRD Spectra of  $Z_{0.25}:S_{0.75}/glass$ .

Finally in Fig. 6, which represents mixing ratio of salts (0% for zinc oxide and 100% for tin oxide).  $SnO_2$  pattern of film was much with standard card (JCPDS No.41-1445) have tetragonal rutile structure, no characteristic peaks for any other oxides or impurities were

observed, suggesting sample have high purity oxide. The highest peak at ( $2\theta=26.5586$ ) for (110). Zinc stannate oxides has been grown on glass substrate with different mixing ratio under invariant condition, typical SEM images was studied. There are no detectable cracks or pores in the films structure, the film morphology depends strongly on the purity and nature of the used precursor.

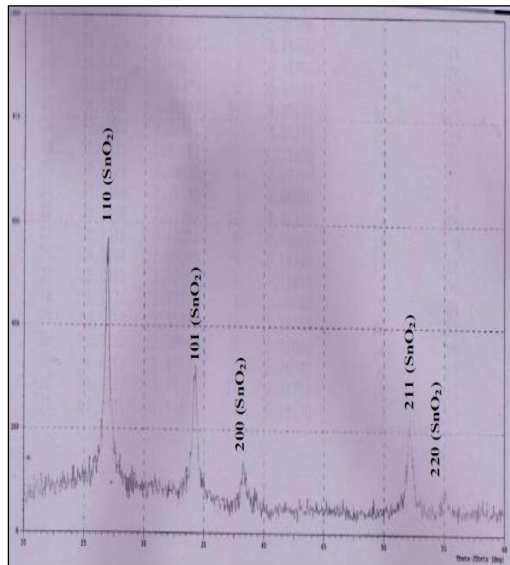


Fig.6 XRD Spectra of  $Zn_0S_1/glass$ .

Fig. 7 shows ZnO (2D-images), the film deposited with zinc is formed a hexagonal, this is consistent with XRD analysis. The latter corresponds to the diffraction plane (002) in the hexagonal Wurtzite structure of ZnO. The appearance of the preferential diffraction peak, assigned to the plane (002), indicates that the film growth is achieved along the axis c of the hexagonal structure normal to the substrate surface Fig.7, this is good concordance with the SEM observation for (Lehraki et al) [20]. The ortho stable form of zinc stannate ( $Zn_2SnO_4$ ) have tri-symmetric face-center cubic spinel structure, SEM (2-D) images for growth  $Zn_2SnO_4$  show the morphology of microcubes at different magnifications Fig. 8, this is good

concordance with the SEM observation for (Baruah and Dutta) [8]. SEM (2-D) images for growth  $Zn_2SnO_4$  and  $ZnSnO_3$  microcubes at different magnifications are shown in Fig. 9.

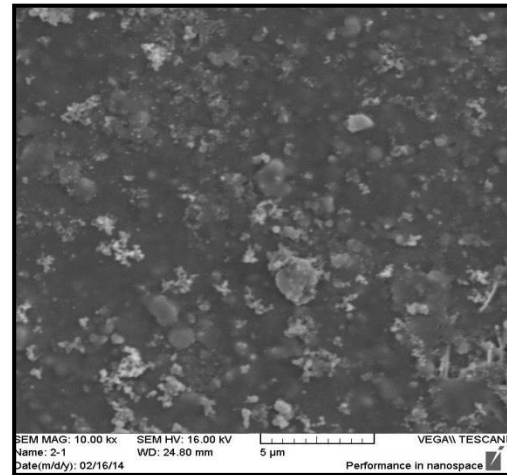


Fig. 7: (SEM) micrograph image for  $Zn_1S_0$ .

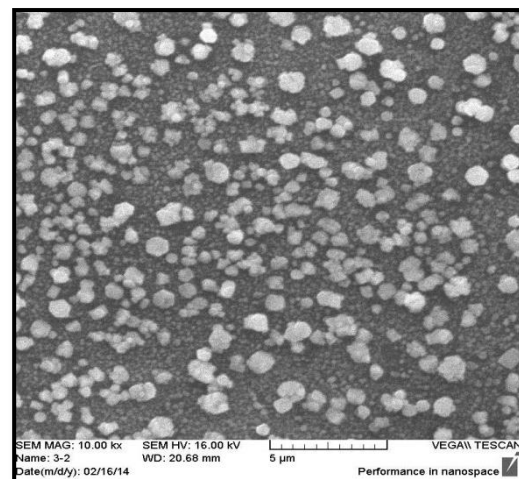


Fig.8: (SEM) micrograph images for  $Zn_{0.75}S_{0.25}$ .

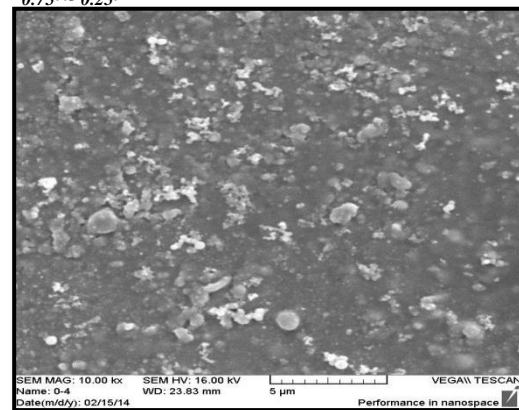


Fig. 9: (SEM) micrograph images for  $Zn_{0.5}S_{0.5}$ .

Zinc stannate ( $ZnSnO_3$ ) has either structure perovskite, according to results XRD the structure was perovskite which shows almost all the particles are spherical in shape leaving some space between them Fig. 10, this is good concordance with the SEM observation for (Singh et al.) [21]. SEM (2D-images) obtained for  $Z_0:S_1$  represented by  $SnO_2$  pure film for sensor application are shown in Fig. 11, summarizes SEM analysis of the  $SnO_2$  deposit have a large area from the surface of the deposit is homogeneous [17].

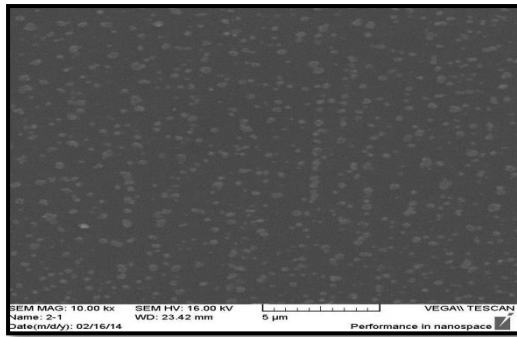


Fig.10: (SEM) micrograph images for  $Z_{0.25}:S_{0.75}$ .

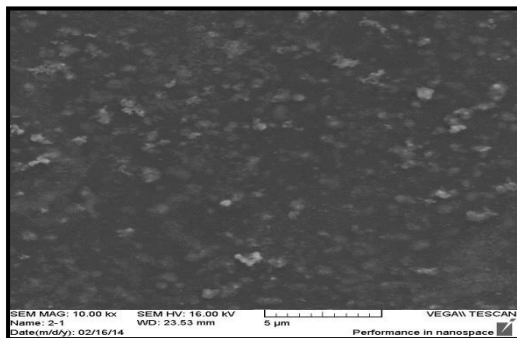


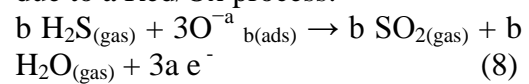
Fig. 11: (SEM) micrograph images for  $Z_0:S_1$ .

AFM is a powerful technique to investigate the surface morphology at nano to microscale. The surface of the films were shown in Figs.12, 13, 14, 15 and 16) for mixing 100, 75, 50, 25, 0% of Z respectively. Irregularities in the film surface (top view) from the spray technique, which benefited tremendously for the gas sensing properties [22]. The (3-D) AFM

micrograph Figs. 12, 13, 14, 15, 16 confirms that the grains are uniformly distributed within the scanning area  $2014 \text{ nm} \times 2014 \text{ nm}$ . This surface characteristic is important for applications gas sensors [23]. In Fig.12, for ZnO the roughness was found 19.62 nm and Avg. diameter 76.06 nm. In Fig.13, for  $Zn_2SnO_4$  the roughness 18.14 nm and Average diameter 91.33 nm, and in Fig.14, for ( $Zn_2SnO_4$  and  $ZnSnO_3$ ) the roughness was found 6.72 nm and Average diameter 109.99 nm, Fig.15 shows  $ZnSnO_3$  surface with roughness was found 4.80 nm and Avg. diameter 81.20 nm and at last fig.16 shows surface morphology of  $SnO_2$  with roughness 22.94 nm and Avg. diameter 68.31 nm. The best value of roughness for higher value last one.

From the above it is clear that all the films were crystalline and was higher for pure binary than the ternary.

For the investigation of the gas sensing properties of the Z:S Oxide films, the optimum operation gas temperature should be fixed initially. Fig. 17, it can be seen that increasing the response of sensor by increased gas concentration on the one hand and un-increased in response with variation of Z:S mixed ratios, which resulted in change oxides consisting as it was seen in XRD results. In the presence of  $H_2S$  in air the sample's resistance decreases due to a Red/Ox process:



where :

$H_2S_{(gas)}$  : is the  $H_2S$  molecule in the gas phase,

$O^{-a}_{b(ads)}$  : an atomic or molecular form of chemisorbed oxygen.

$e^-$  : an electron release, that is injected into the conduction band of the semiconductor.

$SO_{2(gas)}$ ,  $H_2O_{(gas)}$  : the molecular reaction products desorbed from the surface.

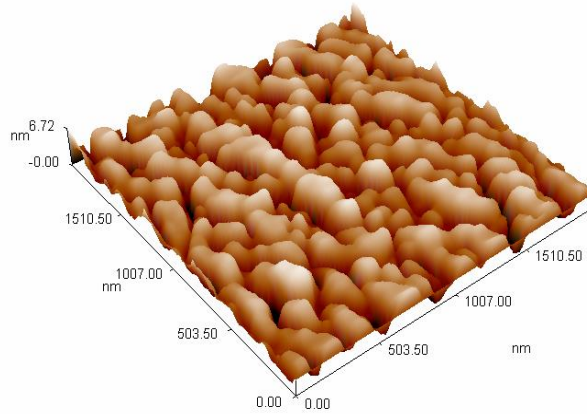
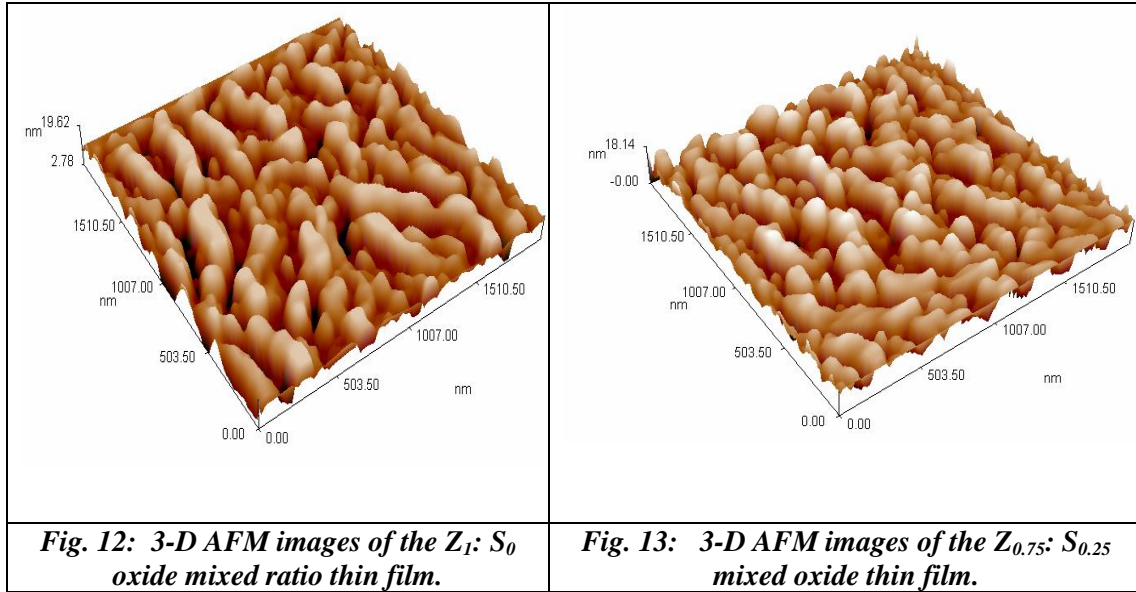
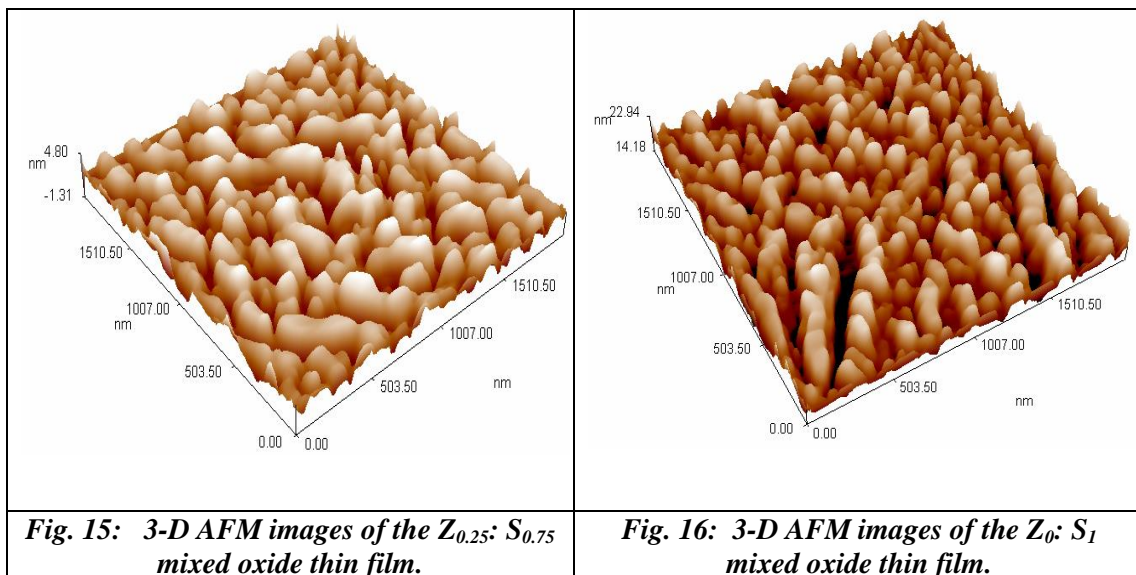


**Fig. 14:** 3-D AFM images of the  $Z_{0.5}: S_{0.5}$  mixed oxide thin film.



Hydrogen sulfide is a Bronsted acid, i.e. heterolytic cleavage of the (S- H) bond is quite easy, especially in the

formation of new donor-acceptor bonds. An increase in  $H_2S$  adsorption on the surface of Z:S oxide can be

achieved with the introduction of modifiers that increase the electron-donor ability of surface basic centers (oxygen anions) [24-25].

Growth of acidity of the ZnO and SnO<sub>2</sub> surface has the opposite effect causing difficulties for a heterolytic break of the (H-S) bond in the H<sub>2</sub>S molecule and a decrease of the H<sub>2</sub>S adsorption.

For other oxides Z:S mixed ratios formed increased response with

increasing oxygen in ZnSnO<sub>3</sub> and Zn<sub>2</sub>SnO<sub>4</sub> oxides, by an increase in H<sub>2</sub>S adsorption on the surface of film oxide can be achieved with the increase the electron (oxygen anions), increase the efficiency of the reaction and the concentration of reactants. For mixed oxides, in addition to the effects of structure, it have higher response comparing with other formed oxides as explained above.

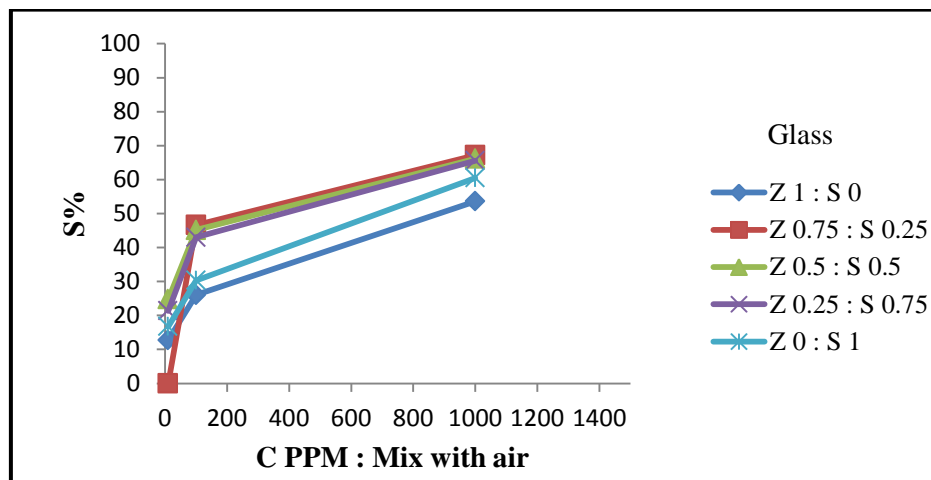


Fig. 17: Gas sensitivity of H<sub>2</sub>S at different mixed.

It can be observed that sensors of ZnO and SnO<sub>2</sub> show relatively low response at the same operating temperature in the range from (10 – 1000) ppm, with the maximum response of 71.5% and 80.61% for ZnO and SnO<sub>2</sub>, at 1000 ppm respectively. Will sensor with mixed oxides (Zn<sub>2</sub>SnO<sub>4</sub>, ZnSnO<sub>3</sub>) exhibits an increase of response to reach the maximum value of 89.57% at the 1000 pm concentration of H<sub>2</sub>S gas for them [25,26]. Fig.18 shows the Response time as a function of gas concentration, it can be seen that the time diminish by increased gas concentration. And it is higher for pure oxide and fewer for mixed oxides. Less response time was 26-10 sec for (10-1000 ppm), starting response times for the pure oxide films (ZnO, SnO<sub>2</sub>)

were estimated to be about 5 sec and for mixed oxide less than 2 sec.

Fig.19 shows that increasing the response of sensors with CH<sub>4</sub> gas concentration increased on the one hand and an increased in response with variation of Z:S Oxide ratio, which resulted in change oxides consisting as it was see in XRD results. It can be observed that sensors based on pristine ZnO and SnO<sub>2</sub> show relatively low response at the operating temperature in the range from 10-1000 ppm, with the maximum response of 35.83 % and 40.18 % for ZnO and SnO<sub>2</sub> at 1000 ppm, respectively. In contrast, sensor with mixed oxides Zn<sub>2</sub>SnO<sub>4</sub>, ZnSnO<sub>3</sub> exhibits an increase of response to reach the maximum value of 45% at the 1000 pm concentration of CH<sub>4</sub> gas for them.

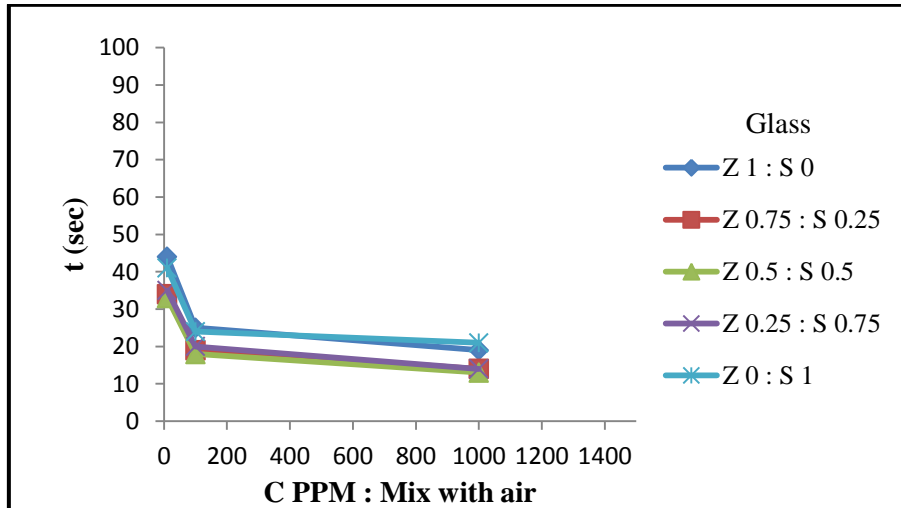


Fig. 18: Response time of Z:S mixed ratio for H<sub>2</sub>S gas.

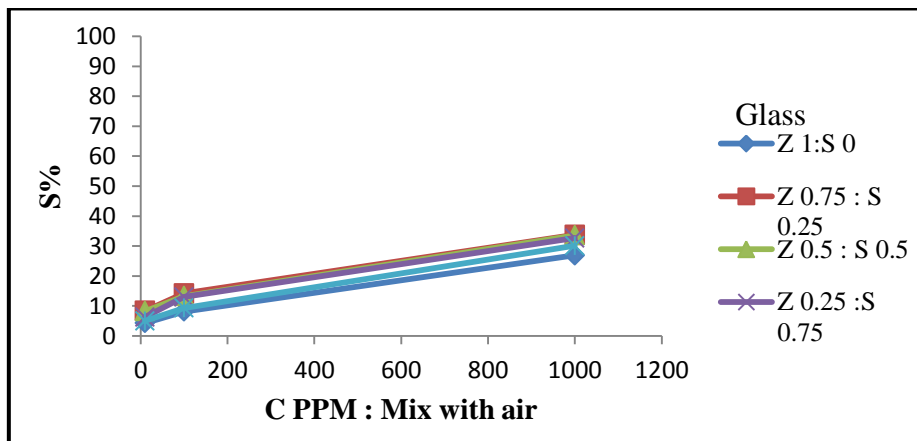


Fig. 19: Gas sensitivity of CH<sub>4</sub> at different mixed ratio.

Fig.20 shows the Response time as a function of gas concentration, it can be seen that the time diminish by increased gas concentration. And it is higher for pure oxide and fewer for mixed oxides. Less response time was 23-12 sec for (10-1000 ppm), starting response times for the pure oxide films (ZnO, SnO<sub>2</sub>) were estimated to be about 6 sec and for mixed oxide less than 3 sec.

In Fig.21, appear that increasing the response of sensors by increased LPG gas concentration on the one hand and an increased in response with variation of Zn:Sn oxide ratio, which resulted in change oxides consisting as it was seen in XRD results. It can be observed that sensors based on pristine ZnO and

SnO<sub>2</sub> show relatively low response at the operating temperature in the range from 10 - 1000 ppm, with the maximum response of 15.7 % and 16.01 % for ZnO and SnO<sub>2</sub> at 1000 ppm, respectively. In contrast, sensor with mixed oxides Zn<sub>2</sub>SnO<sub>4</sub> and ZnSnO<sub>3</sub>) exhibits an increase of response to reach the maximum value of 20.8% at the 1000 ppm concentration of LPG gas for them. Fig.22 shows the response time as a function of gas concentration, it can be seen that the time diminish by increased gas concentration [26,27]. And it is higher for pure oxide and fewer for mixed oxides. Less response time was 33-22sec for 10-1000 ppm, starting response times for the pure oxide films ZnO, SnO<sub>2</sub> were estimated to be about

4 sec and for mixed oxide less than 2sec.

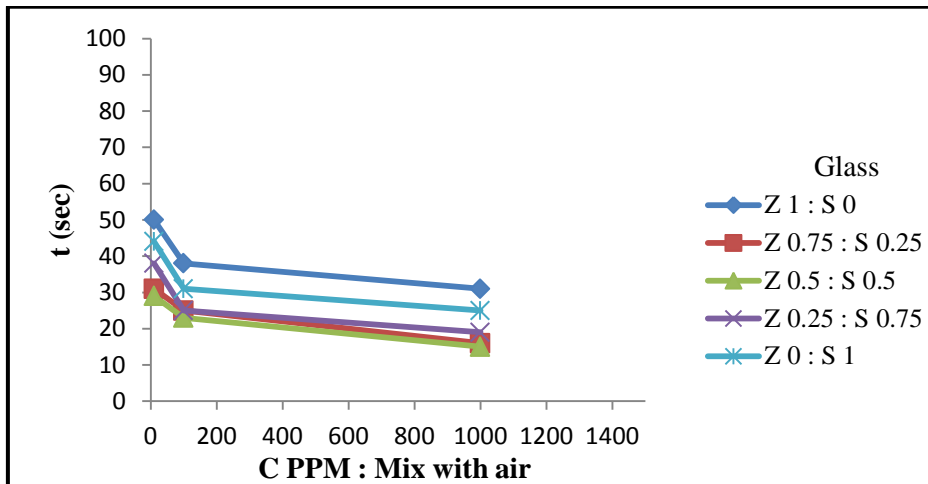


Fig. 20: Response time of Z:S mixed ratio for CH<sub>4</sub> gas.

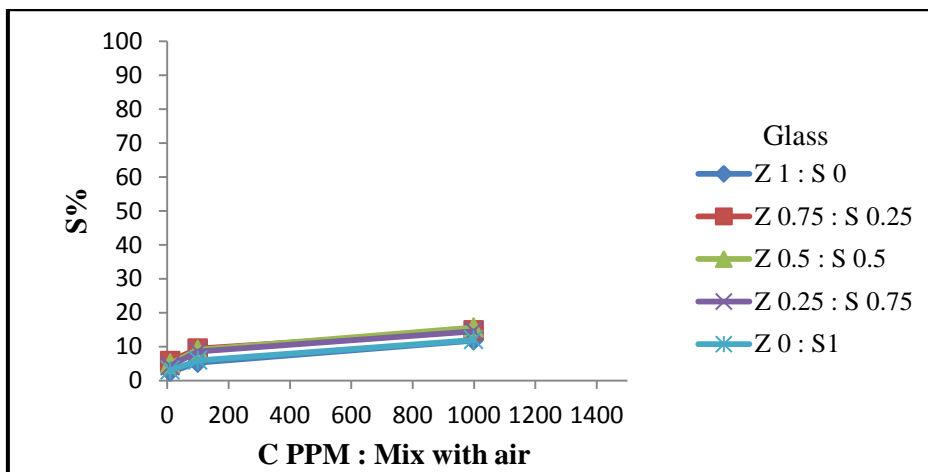


Fig. 21: Gas sensitivity of LPG at different mixed ratio.

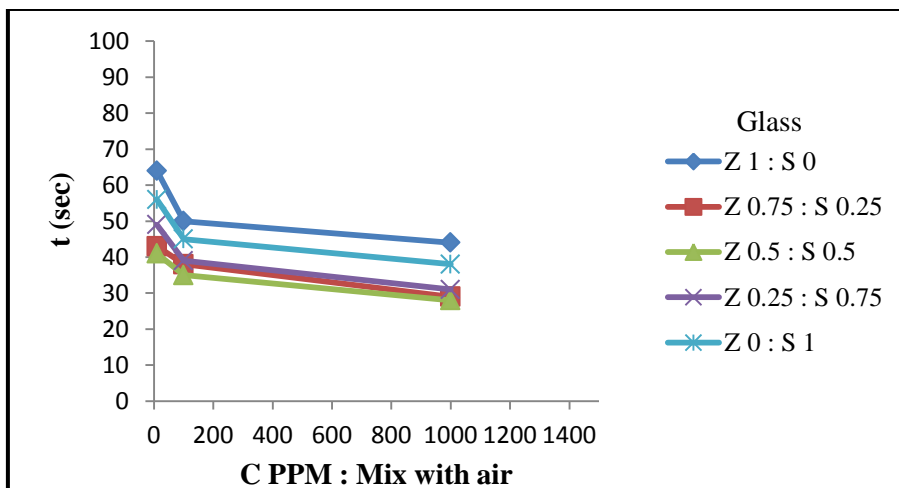


Fig. 22: Response time of Z:S mixed ratio for LPG gas.

**Conclusions**

Build an sensor with several oxides form of ZnO, Zn<sub>2</sub>SnO<sub>4</sub>, ZnSnO<sub>3</sub>, SnO<sub>2</sub>

on glass substrates to detect different reduction gases.

Mixing ratios chloride salts generate different oxide compounds ternary and binary with different responses for different testing reduction gases. All thin films shows homogenous surface and crystalline structures; hexagonal, tetragonal and cubic for oxides ZnO, SnO<sub>2</sub>, ZnSnO<sub>3</sub> and Zn<sub>2</sub>SnO<sub>4</sub> respectively, all the films were crystalline and was higher for binary than the ternary. Mixing oxides Zn<sub>2</sub>SnO<sub>4</sub> and ZnSnO<sub>3</sub> showed the highest response rate for all testing gases at the best possible time, while the best crystallization were for binary oxides. Sensitivity for H<sub>2</sub>S, CH<sub>4</sub> and LPG gases were about 80, 35 and 15% respectively and response time around 10, 12 and 22 sec respectively for the binary oxides. While for the mixed ternary oxides for the gases were 89, 45 and 20 % and response time of (5-2), (6-3) and (4-2) sec respectively.

### References

- [1] G. Neri, Recent Patents on Materials Science, 4 (2011) 146-158.
- [2] G. Korotcenkov, Materials Science and Engineering B, 139 (2007) 1–23.
- [3] K. Zakrzewska, Thin Solid Films, 391(2001) 229-238.
- [4] A. Chowdhuri, V. Gupta, K.Sreenives, Applied Physics Letters, 84, 7 (2004) 1181-1182.
- [5] J. Gong, Q. Chen, W. Fei, S. Seal, Sensors and Actuators B., 102 (2004) 117–125.
- [6] M. Batzill, U. Diebold, Progress in Surface Science, 79 (2005) 47–154,
- [7] Cleveland, Ohio, CRC handbook of Chemistry and Physics 1978.
- [8] S. Baruah, J. Dutta, Sci. Technol. Adv. Mater., 12 (2011) 18.
- [9] L.A. Patil, I.G. Pathan, Procedia Materials Science, 6 (2014)1557-1565.
- [10] P. Patnaik, Handbook of Inorganic Chemicals, McGraw-Hill, (2003).
- [11] M. Kojim, "The role of liquefied petroleum gas in reducing energy poverty", Extractive industrial for Development Series, Vol. 25, (2011).
- [12] C. Woong, S.Park and J. Lee, B: Chemical J., Sensors and Actuators, B174 (2012) 495– 499.
- [13] S. Lee, S. Kim, B. Hwang, S. Jung, D. Ragupathy, Sensors, 13 (2013) 3889-3901.
- [14] C.M. Mahajan, Current Applied Physics, 13, 9 (2013) 2109–2116.
- [15] V.R. Shinde, Sensors and actuators B: Chemical, 120 (2007) 551–559.
- [16] K. Jeyadheepan, C. Sanjeeviraja, Journal of Chemistry, ID 245918, (2014).
- [17] A. Salehi, M. Gholizade, Sensor and Actuators B, 89 (2003) 173-179.
- [18] M. Miyauchi, Z. Liu, Z. Zhao, S. Anandan, K. Hara, Chemical Communications, 46 (2010) 1529-1532.
- [19] S. V. Ryabtsev, E. P. Domashevskaya, E. P. Domashevskaya, Condensed Matter and Interphase Boundaries, 12, 1 (2010) 17-21.
- [20] N. Lehraki, M.S. Aida, S. Abed, N. Attaf, A. Attaf and M. Poulain, Current Applied Physics, 12 (2012)1-5.
- [21] R. Singh, A. K. Yadav, C. Gautam, Journal of Sensor Technology, 1 (2011) 116-124.
- [22] Y.C. Ji, H.X. Zhang, X. H. Zhang, Z. Q. Li., Cond-Mat. Mtrl-Sci, 1, (2013) 2-7.
- [23] Q. G. Hial, "Improvement of ZnO and SnO<sub>2</sub> hydrogen gas sensors", Ph.D Thesis, University of Technology (2011).
- [24] T. Akamatsu, T. Itoh, N. Izu, W. Shin, Sensors, 13 (2013) 12467-12481.
- [25] G. Ma, R. Zou, "Cryst. Eng. Comm., 14 (2012) 2172-2179.
- [26] F.N. Jiménez-García, C.L. Londoño-Calderón, D.G. Espinosa-Arbeláez, A. del Real, M. E. Rodríguez-García, Journal of physics

and Chemistry of Solids, 68, (2007)  
1981-1988 .

[27] Ghosh, Jadavpur and Basak,  
Journal of Applied Physics, 96 (2004)  
2689 – 2692.